Fermilab-Pub-08/061-E

Search for large extra dimensions in the mono-photon final state at $\sqrt{s} = 1.96$ TeV

V.M. Abazov[36], B. Abbott[75], M. Abolins[65], B.S. Acharya[29], M. Adams[51], T. Adams[49], E. Aguilo[6], S.H. Ahn[31], M. Ahsan[59], G.D. Alexeev[36], G. Alkhazov[40], A. Alton[64,a], G. Alverson[63], G.A. Alves[2], M. Anastasoaie[35], L.S. Ancu[35], T. Andeen[53], S. Anderson[45], B. Andrieu[17], M.S. Anzelc[53], M. Aoki[50], Y. Arnoud[14], M. Arov[60], M. Arthaud[18], A. Askew[49], B. Åsman[41], A.C.S. Assis Jesus[3], O. Atramentov[49], C. Avila[8], C. Ay[24], F. Badaud[13], A. Baden[61], L. Bagby[50], B. Baldin[50], D.V. Bandurin[59], P. Banerjee[29], S. Banerjee[29], E. Barberis[63], A.-F. Barfuss[15], P. Bargassa[80], P. Baringer[58], J. Barreto[2], J.F. Bartlett[50], U. Bassler[18], D. Bauer[43], S. Beale[6], A. Bean[58], M. Begalli[3], M. Begel[73], C. Belanger-Champagne[41], L. Bellantoni[50], A. Bellavance[50], J.A. Benitez[65], S.B. Beri[27], G. Bernardi[17], R. Bernhard[23], I. Bertram[42], M. Besançon[18], R. Beuselinck[43], V.A. Bezzubov[39], P.C. Bhat[50], V. Bhatnagar[27], C. Biscarat[20], G. Blazey[52], F. Blekman[43], S. Blessing[49], D. Bloch[19], K. Bloom[67], A. Boehnlein[50], D. Boline[62], T.A. Bolton[59], G. Borissov[42], T. Bose[77], A. Brandt[78], R. Brock[65], G. Brooijmans[70], A. Bross[50], D. Brown[81], N.J. Buchanan[49], D. Buchholz[53], M. Buehler[81], V. Buescher[22], V. Bunichev[38], S. Burdin[42,b], S. Burke[45], T.H. Burnett[82], C.P. Buszello[43], J.M. Butler[62], P. Calfayan[25], S. Calvet[16], J. Cammin[71], E. Carrera[49], W. Carvalho[3], B.C.K. Casey[50], H. Castilla-Valdez[33], S. Chakrabarti[18], D. Chakraborty[52], K. Chan[6], K.M. Chan[55], A. Chandra[48], F. Charles[19,‡], E. Cheu[45], F. Chevallier[14], D.K. Cho[62], S. Choi[32], B. Choudhary[28], L. Christofek[77], T. Christoudias[43], S. Cihangir[50], D. Claes[67], Y. Coadou[6], M. Cooke[80], W.E. Cooper[50], M. Corcoran[80], F. Couderc[18], M.-C. Cousinou[15], S. Crépé-Renaudin[14], D. Cutts[77], M. Ćwiok[30], H. da Motta[2], A. Das[45], G. Davies[43], K. De[78], S.J. de Jong[35], E. De La Cruz-Burelo[64], C. De Oliveira Martins[3], J.D. Degenhardt[64], F. Déliot[18], M. Demarteau[50], R. Demina[71], D. Denisov[50], S.P. Denisov[39], S. Desai[50], H.T. Diehl[50], M. Diesburg[50], A. Dominguez[67], H. Dong[72], L.V. Dudko[38], L. Duflot[16], S.R. Dugad[29], D. Duggan[49], A. Duperrin[15], J. Dyer[65], A. Dyshkant[52], M. Eads[67], D. Edmunds[65], J. Ellison[48], V.D. Elvira[50], Y. Enari[77], S. Eno[61], P. Ermolov[38], H. Evans[54], A. Evdokimov[73], V.N. Evdokimov[39], A.V. Ferapontov[59], T. Ferbel[71], F. Fiedler[24], F. Filthaut[35], W. Fisher[50], H.E. Fisk[50], M. Fortner[52], H. Fox[42], S. Fu[50], S. Fuess[50], T. Gadfort[70], C.F. Galea[35], E. Gallas[50], C. Garcia[71], A. Garcia-Bellido[82], V. Gavrilov[37], P. Gay[13], W. Geist[19], D. Gelé[19], C.E. Gerber[51], Y. Gershtein[49], D. Gillberg[6], G. Ginther[71], N. Gollub[41], B. Gómez[8], A. Goussiou[82], P.D. Grannis[72], H. Greenlee[50], Z.D. Greenwood[60], E.M. Gregores[4], G. Grenier[20], Ph. Gris[13], J.-F. Grivaz[16], A. Grohsjean[25], S. Grünendahl[50], M.W. Grünewald[30], F. Guo[72], J. Guo[72], G. Gutierrez[50], P. Gutierrez[75], A. Haas[70], N.J. Hadley[61], P. Haefner[25], S. Hagopian[49], J. Haley[68], I. Hall[65], R.E. Hall[47], L. Han[7], K. Harder[44], A. Harel[71], R. Harrington[63], J.M. Hauptman[57], R. Hauser[65], J. Hays[43], T. Hebbeker[21], D. Hedin[52], J.G. Hegeman[34], J.M. Heinmiller[51], A.P. Heinson[48], U. Heintz[62], C. Hensel[58], K. Herner[72], G. Hesketh[63], M.D. Hildreth[55], R. Hirosky[81], J.D. Hobbs[72], B. Hoeneisen[12], H. Hoeth[26], M. Hohlfeld[22], S.J. Hong[31], S. Hossain[75], P. Houben[34], Y. Hu[72], Z. Hubacek[10], V. Hynek[9], I. Iashvili[69], R. Illingworth[50], A.S. Ito[50], S. Jabeen[62], M. Jaffré[16], S. Jain[75], K. Jakobs[23], C. Jarvis[61], R. Jesik[43], K. Johns[45], C. Johnson[70], M. Johnson[50], A. Jonckheere[50], P. Jonsson[43], A. Juste[50], E. Kajfasz[15], A.M. Kalinin[36], J.M. Kalk[60], S. Kappler[21], D. Karmanov[38], P.A. Kasper[50], I. Katsanos[70], D. Kau[49], V. Kaushik[78], R. Kehoe[79], S. Kermiche[15], N. Khalatyan[50], A. Khanov[76], A. Kharchilava[69], Y.M. Kharzheev[36], D. Khatidze[70], T.J. Kim[31], M.H. Kirby[53], M. Kirsch[21], B. Klima[50], J.M. Kohli[27], J.-P. Konrath[23], V.M. Korablev[39], A.V. Kozelov[39], J. Kraus[65], D. Krop[54], T. Kuhl[24], A. Kumar[69], A. Kupco[11], T. Kurča[20], J. Kvita[9], F. Lacroix[13], D. Lam[55], S. Lammers[70], G. Landsberg[77], P. Lebrun[20], W.M. Lee[50], A. Leflat[38], J. Lellouch[17], J. Leveque[45], J. Li[78], L. Li[48], Q.Z. Li[50], S.M. Lietti[5], J.G.R. Lima[52], D. Lincoln[50], J. Linnemann[65], V.V. Lipaev[39], R. Lipton[50], Y. Liu[7], Z. Liu[6], A. Lobodenko[40], M. Lokajicek[11], P. Love[42], H.J. Lubatti[82], R. Luna[3], A.L. Lyon[50], A.K.A. Maciel[2], D. Mackin[80], R.J. Madaras[46], P. Mättig[26], C. Magass[21], A. Magerkurth[64], P.K. Mal[82], H.B. Malbouisson[3], S. Malik[67], V.L. Malyshev[36], H.S. Mao[50], Y. Maravin[59], B. Martin[14], R. McCarthy[72], A. Melnitchouk[66], L. Mendoza[8], P.G. Mercadante[5], M. Merkin[38], K.W. Merritt[50], A. Meyer[21], J. Meyer[22,d], T. Millet[20], J. Mitrevski[70], J. Molina[3], R.K. Mommsen[44], N.K. Mondal[29], R.W. Moore[6], T. Moulik[58], G.S. Muanza[20], M. Mulders[50], M. Mulhearn[70], O. Mundal[22], L. Mundim[3], E. Nagy[15], M. Naimuddin[50], M. Narain[77], N.A. Naumann[35], H.A. Neal[64], J.P. Negret[8], P. Neustroev[40], H. Nilsen[23], H. Nogima[3], S.F. Novaes[5], T. Nunnemann[25], V. O'Dell[50], D.C. O'Neil[6], G. Obrant[40], C. Ochando[16], D. Onoprienko[59], N. Oshima[50], N. Osman[43], J. Osta[55], R. Otec[10], G.J. Otero y Garzón[50], M. Owen[44], P. Padley[80], M. Pangilinan[77], N. Parashar[56], S.-J. Park[71], S.K. Park[31],

J. Parsons[70], R. Partridge[77], N. Parua[54], A. Patwa[73], G. Pawloski[80], B. Penning[23], M. Perfilov[38], K. Peters[44], Y. Peters[26], P. Pétroff[16], M. Petteni[43], R. Piegaia[1], J. Piper[65], M.-A. Pleier[22], P.L.M. Podesta-Lerma[33,c], V.M. Podstavkov[50], Y. Pogorelov[55], M.-E. Pol[2], P. Polozov[37], B.G. Pope[65], A.V. Popov[39], C. Potter[6], W.L. Prado da Silva[3], H.B. Prosper[49], S. Protopopescu[73], J. Qian[64], A. Quadt[22,d], B. Quinn[66], A. Rakitine[42], M.S. Rangel[2], K. Ranjan[28], P.N. Ratoff[42], P. Renkel[79], S. Reucroft[63], P. Rich[44], J. Rieger[54], M. Rijssenbeek[72], I. Ripp-Baudot[19], F. Rizatdinova[76], S. Robinson[43], R.F. Rodrigues[3], M. Rominsky[75], C. Royon[18], P. Rubinov[50], R. Ruchti[55], G. Safronov[37], G. Sajot[14], A. Sánchez-Hernández[33], M.P. Sanders[17], A. Santoro[3], G. Savage[50], L. Sawyer[60], T. Scanlon[43], D. Schaile[25], R.D. Schamberger[72], Y. Scheglov[40], H. Schellman[53], T. Schliephake[26], C. Schwanenberger[44], A. Schwartzman[68], R. Schwienhorst[65], J. Sekaric[49], H. Severini[75], E. Shabalina[51], M. Shamim[59], V. Shary[18], A.A. Shchukin[39], R.K. Shivpuri[28], V. Siccardi[19], V. Simak[10], V. Sirotenko[50], P. Skubic[75], P. Slattery[71], D. Smirnov[55], G.R. Snow[67], J. Snow[74], S. Snyder[73], S. Söldner-Rembold[44], L. Sonnenschein[17], A. Sopczak[42], M. Sosebee[78], K. Soustruznik[9], B. Spurlock[78], J. Stark[14], J. Steele[60], V. Stolin[37], D.A. Stoyanova[39], J. Strandberg[64], S. Strandberg[41], M.A. Strang[69], E. Strauss[72], M. Strauss[75], R. Ströhmer[25], D. Strom[53], L. Stutte[50], S. Sumowidagdo[49], P. Svoisky[55], A. Sznajder[3], P. Tamburello[45], A. Tanasijczuk[1], W. Taylor[6], J. Temple[45], B. Tiller[25], F. Tissandier[13], M. Titov[18], V.V. Tokmenin[36], T. Toole[61], I. Torchiani[23], T. Trefzger[24], D. Tsybychev[72], B. Tuchming[18], C. Tully[68], P.M. Tuts[70], R. Unalan[65], L. Uvarov[40], S. Uvarov[40], S. Uzunyan[52], B. Vachon[6], P.J. van den Berg[34], R. Van Kooten[54], W.M. van Leeuwen[34], N. Varelas[51], E.W. Varnes[45], I.A. Vasilyev[39], M. Vaupel[26], P. Verdier[20], L.S. Vertogradov[36], M. Verzocchi[50], F. Villeneuve-Seguier[43], P. Vint[43], P. Vokac[10], E. Von Toerne[59], M. Voutilainen[68,e], R. Wagner[68], H.D. Wahl[49], L. Wang[61], M.H.L.S. Wang[50], J. Warchol[55], G. Watts[82], M. Wayne[55], G. Weber[24], M. Weber[50], L. Welty-Rieger[54], A. Wenger[23,f], N. Wermes[22], M. Wetstein[61], A. White[78], D. Wicke[26], G.W. Wilson[58], S.J. Wimpenny[48], M. Wobisch[60], D.R. Wood[63], T.R. Wyatt[44], Y. Xie[77], S. Yacoob[53], R. Yamada[50], M. Yan[61], T. Yasuda[50], Y.A. Yatsunenko[36], K. Yip[73], H.D. Yoo[77], S.W. Youn[53], J. Yu[78], A. Zatserklyaniy[52], C. Zeitnitz[26], T. Zhao[82], B. Zhou[64], J. Zhu[72], M. Zielinski[71], D. Zieminska[54], A. Zieminski[54,‡], L. Zivkovic[70], V. Zutshi[52], and E.G. Zverev[38]

(The DØ Collaboration)

[1]*Universidad de Buenos Aires, Buenos Aires, Argentina*
[2]*LAFEX, Centro Brasileiro de Pesquisas Físicas, Rio de Janeiro, Brazil*
[3]*Universidade do Estado do Rio de Janeiro, Rio de Janeiro, Brazil*
[4]*Universidade Federal do ABC, Santo André, Brazil*
[5]*Instituto de Física Teórica, Universidade Estadual Paulista, São Paulo, Brazil*
[6]*University of Alberta, Edmonton, Alberta, Canada, Simon Fraser University, Burnaby, British Columbia, Canada, York University, Toronto, Ontario, Canada, and McGill University, Montreal, Quebec, Canada*
[7]*University of Science and Technology of China, Hefei, People's Republic of China*
[8]*Universidad de los Andes, Bogotá, Colombia*
[9]*Center for Particle Physics, Charles University, Prague, Czech Republic*
[10]*Czech Technical University, Prague, Czech Republic*
[11]*Center for Particle Physics, Institute of Physics, Academy of Sciences of the Czech Republic, Prague, Czech Republic*
[12]*Universidad San Francisco de Quito, Quito, Ecuador*
[13]*LPC, Univ Blaise Pascal, CNRS/IN2P3, Clermont, France*
[14]*LPSC, Université Joseph Fourier Grenoble 1, CNRS/IN2P3, Institut National Polytechnique de Grenoble, France*
[15]*CPPM, IN2P3/CNRS, Université de la Méditerranée, Marseille, France*
[16]*LAL, Univ Paris-Sud, IN2P3/CNRS, Orsay, France*
[17]*LPNHE, IN2P3/CNRS, Universités Paris VI and VII, Paris, France*
[18]*DAPNIA/Service de Physique des Particules, CEA, Saclay, France*
[19]*IPHC, Université Louis Pasteur et Université de Haute Alsace, CNRS/IN2P3, Strasbourg, France*
[20]*IPNL, Université Lyon 1, CNRS/IN2P3, Villeurbanne, France and Université de Lyon, Lyon, France*
[21]*III. Physikalisches Institut A, RWTH Aachen, Aachen, Germany*
[22]*Physikalisches Institut, Universität Bonn, Bonn, Germany*
[23]*Physikalisches Institut, Universität Freiburg, Freiburg, Germany*
[24]*Institut für Physik, Universität Mainz, Mainz, Germany*
[25]*Ludwig-Maximilians-Universität München, München, Germany*
[26]*Fachbereich Physik, University of Wuppertal, Wuppertal, Germany*
[27]*Panjab University, Chandigarh, India*

[28]*Delhi University, Delhi, India*
[29]*Tata Institute of Fundamental Research, Mumbai, India*
[30]*University College Dublin, Dublin, Ireland*
[31]*Korea Detector Laboratory, Korea University, Seoul, Korea*
[32]*SungKyunKwan University, Suwon, Korea*
[33]*CINVESTAV, Mexico City, Mexico*
[34]*FOM-Institute NIKHEF and University of Amsterdam/NIKHEF, Amsterdam, The Netherlands*
[35]*Radboud University Nijmegen/NIKHEF, Nijmegen, The Netherlands*
[36]*Joint Institute for Nuclear Research, Dubna, Russia*
[37]*Institute for Theoretical and Experimental Physics, Moscow, Russia*
[38]*Moscow State University, Moscow, Russia*
[39]*Institute for High Energy Physics, Protvino, Russia*
[40]*Petersburg Nuclear Physics Institute, St. Petersburg, Russia*
[41]*Lund University, Lund, Sweden, Royal Institute of Technology and Stockholm University, Stockholm, Sweden, and Uppsala University, Uppsala, Sweden*
[42]*Lancaster University, Lancaster, United Kingdom*
[43]*Imperial College, London, United Kingdom*
[44]*University of Manchester, Manchester, United Kingdom*
[45]*University of Arizona, Tucson, Arizona 85721, USA*
[46]*Lawrence Berkeley National Laboratory and University of California, Berkeley, California 94720, USA*
[47]*California State University, Fresno, California 93740, USA*
[48]*University of California, Riverside, California 92521, USA*
[49]*Florida State University, Tallahassee, Florida 32306, USA*
[50]*Fermi National Accelerator Laboratory, Batavia, Illinois 60510, USA*
[51]*University of Illinois at Chicago, Chicago, Illinois 60607, USA*
[52]*Northern Illinois University, DeKalb, Illinois 60115, USA*
[53]*Northwestern University, Evanston, Illinois 60208, USA*
[54]*Indiana University, Bloomington, Indiana 47405, USA*
[55]*University of Notre Dame, Notre Dame, Indiana 46556, USA*
[56]*Purdue University Calumet, Hammond, Indiana 46323, USA*
[57]*Iowa State University, Ames, Iowa 50011, USA*
[58]*University of Kansas, Lawrence, Kansas 66045, USA*
[59]*Kansas State University, Manhattan, Kansas 66506, USA*
[60]*Louisiana Tech University, Ruston, Louisiana 71272, USA*
[61]*University of Maryland, College Park, Maryland 20742, USA*
[62]*Boston University, Boston, Massachusetts 02215, USA*
[63]*Northeastern University, Boston, Massachusetts 02115, USA*
[64]*University of Michigan, Ann Arbor, Michigan 48109, USA*
[65]*Michigan State University, East Lansing, Michigan 48824, USA*
[66]*University of Mississippi, University, Mississippi 38677, USA*
[67]*University of Nebraska, Lincoln, Nebraska 68588, USA*
[68]*Princeton University, Princeton, New Jersey 08544, USA*
[69]*State University of New York, Buffalo, New York 14260, USA*
[70]*Columbia University, New York, New York 10027, USA*
[71]*University of Rochester, Rochester, New York 14627, USA*
[72]*State University of New York, Stony Brook, New York 11794, USA*
[73]*Brookhaven National Laboratory, Upton, New York 11973, USA*
[74]*Langston University, Langston, Oklahoma 73050, USA*
[75]*University of Oklahoma, Norman, Oklahoma 73019, USA*
[76]*Oklahoma State University, Stillwater, Oklahoma 74078, USA*
[77]*Brown University, Providence, Rhode Island 02912, USA*
[78]*University of Texas, Arlington, Texas 76019, USA*
[79]*Southern Methodist University, Dallas, Texas 75275, USA*
[80]*Rice University, Houston, Texas 77005, USA*
[81]*University of Virginia, Charlottesville, Virginia 22901, USA and*
[82]*University of Washington, Seattle, Washington 98195, USA*

(Dated: March 14, 2008)

We report on a search for large extra dimensions in a data sample of approximately 1 fb^{-1} of $p\overline{p}$ collisions at $\sqrt{s} = 1.96$ TeV. We investigate Kaluza-Klein graviton production with a photon and missing transverse energy in the final state. At the 95% C.L. we set limits on the fundamental mass scale M_D from 884 GeV to 778 GeV for 2 to 8 extra dimensions.

PACS numbers: 13.85.Rm, 11.10.Kk

Arkani-Hamed, Dimopoulos, and Dvali (ADD) [1] made the first attempt to solve the hierarchy problem of the standard model (SM) by postulating the existence of n new large extra spatial dimensions (LED). In this approach, the SM particles are confined to a 3-dimensional brane while gravity is diluted in the larger volume. The size of the compactified extra space (R), the effective Planck scale in the 4-dimensional space-time (M_{Pl}), and the fundamental Planck scale in the $(4+n)$-dimensional space-time (M_D), are related by the expression $M_{Pl}^2 = 8\pi M_D^{n+2} R^n$. Due to the compactification of the extra space, the gravitational field appears as a series of quantized energy states which are referred as Kaluza-Klein modes with mass splittings $\Delta m \approx 1/R$. For a moderate number of extra dimensions ($n \leq 8$), the mass splitting is small enough that the different modes can be integrated. A Kaluza-Klein graviton (G_{KK}) behaves like a massive, non-interacting, stable particle whose direct production gives an imbalance in the final state momentum as its collider signature.

In this Letter we report the results of a search for LED in $p\overline{p}$ collisions at $\sqrt{s} = 1.96$ TeV, using the D0 detector at the Fermilab Tevatron collider in the exclusive single photon plus missing transverse energy ($\gamma + \not\!\!E_T$) final state. This signature arises from the process $q\overline{q} \to \gamma G_{KK}$ which is studied in detail in [2]. The CDF experiment carried out a similar search with 87 pb^{-1}of data, setting 95% C.L. lower limits on the fundamental Planck scale M_D of 549, 581 and 601 GeV for 4, 6, and 8 extra dimensions, respectively [3]. Several other searches for LED have been performed by collaborations at the Tevatron [4, 5] and the CERN LEP collider [6].

The backgrounds to the $\gamma + \not\!\!E_T$ signal are dominated by electroweak boson production and non-beam collision background where muons from the beam halo or cosmic rays undergo bremsstrahlung producing an energetic photon. The former source is dominated by the $Z + \gamma \to \nu\overline{\nu} + \gamma$ process, followed by $W \to e\nu$ where the electron is misidentified as a photon, $W + \gamma$ where the lepton from the W boson decay is not detected, and $W/Z+$jet production where the jet is misidentified as a photon.

The D0 detector [7] comprises a central-tracking system with a silicon microstrip tracker (SMT) and a central fiber tracker (CFT), both housed within a 2 T superconducting solenoidal magnet, with designs optimized for tracking and vertexing at $|\eta| < 3$ and $|\eta| < 2.5$, respectively, where η is the pseudorapidity [8] measured with respect to the geometrical center of the detector. The central preshower system (CPS) is located in front of a liquid-argon/uranium calorimeter and consists of three layers of scintillating strips, providing precise measurement of EM shower positions. The calorimeter has a central section (CC) covering $|\eta| \leq 1.1$, and two end calorimeters (EC) that extend coverage to $|\eta| \approx 4.2$, each of them located in a separate cryostat [9]. Each calorimeter contains an electromagnetic (EM) section closest to the interaction region followed by fine and coarse hadronic sections. The electromagnetic part has four longitudinal layers and transverse segmentation of 0.1×0.1 in $\eta - \phi$ space (where ϕ is the azimuthal angle), with the exception of the third layer, where it is 0.05×0.05. Additionally, scintillators between the CC and EC cryostats provide sampling of developing showers for $1.1 < |\eta| < 1.4$. The outer muon system, covering $|\eta| < 2$, consists of a layer of tracking detectors and scintillation trigger counters in front of 1.8 T iron toroids, followed by two similar layers after the toroids. The data in this analysis were recorded using single electromagnetic object triggers that are almost 100% efficient to select signal events. It corresponds to an integrated luminosity of 1.05 ± 0.06 fb^{-1} [10].

We identify a reconstructed calorimeter cluster as a photon when it satisfies the following requirements (photon ID): (i) at least 90% of the energy is deposited in the EM section of the calorimeter; (ii) the calorimeter isolation variable $\mathcal{I} = [E_{\rm tot}(0.4) - E_{\rm em}(0.2)]/E_{\rm em}(0.2)$ is less than 0.07, where $E_{\rm tot}(0.4)$ denotes the total energy deposited in the calorimeter in a cone of radius $\mathcal{R} = \sqrt{(\Delta\eta)^2 + (\Delta\phi)^2} = 0.4$, and $E_{\rm em}(0.2)$ is the EM energy in a cone of radius $\mathcal{R} = 0.2$; (iii) the track isolation variable, defined as the scalar sum of the transverse momenta (p_T) of all tracks which originate from the interaction vertex in an annulus of $0.05 < \mathcal{R} < 0.4$ around the cluster, is less than 2 GeV; (iv) it is in the CC with $|\eta| < 1.1$; (v) both transverse and longitudinal shower shapes are consistent with those of a photon; (vi) it has neither an associated track in the central tracking system nor a significant density of hits in the SMT and CFT systems consistent with the presence of a track with p_T in agreement with its transverse energy; and (vii) there is energy depositon in the CPS matched to it. Jets are reconstructed using the iterative midpoint cone algorithm [11] with a cone size of 0.5. The missing transverse energy is computed from calorimeter cells with $|\eta| < 4$ and corrected for the EM and jet energy scales.

The *photon* sample is obtained by selecting events with only one photon with $p_T > 90$ GeV, at least one reconstructed interaction vertex consistent with the measured direction of the photon (see below), and $\not\!\!E_T > 70$ GeV. This high $\not\!\!E_T$ requirement guarantees negligible multijet background in the final candidate sample. Additionally, in order to avoid large $\not\!\!E_T$ due to mismeasurement of jet energy, we require no jets with $p_T > 15$ GeV. We reject events with reconstructed muons and with cosmic ray muons identified by the muon scintillator counters timing signal or by the presence of a characteristic pattern of hits in the muon drift chambers aligned with the reconstructed photon. In order to further reject events with leptons that leave a distinguishable signature in the tracker but that are not reconstructed in the other subsystems of the detector, we impose a requirement on the transverse momentum of any isolated track not to be greater than 6.5 GeV. A track is considered to be isolated if the ratio between the scalar sum of the p_T of all tracks which originate from the interaction vertex in an annulus of $0.1 < \mathcal{R} < 0.4$ around the track and the p_T of the track is less than 0.3.

The EM pointing algorithm allows the calculation of the direction of the EM shower based on the transverse and longitudinal segmentation of the calorimeter and preshower systems. EM pointing is performed independently in the azimuthal and polar planes. The former results in the measurement of the distance of closest approach to the beam line (DCA), and the latter in the prediction of the z position (along the beam) of the interaction vertex in the event. We require that the z coordinate of at least one interaction vertex in the event be within 10 cm of the position predicted by the pointing algorithm, and use the DCA to estimate the remaining backgrounds from jet-photon misidentification and non-collision muons. Misidentified jets have poor pointing resolution, and therefore (compared to electrons or photons) a wider DCA distribution is expected. Likewise, one can anticipate the DCA distribution for non-collision events to have an even wider shape. After these requirements, 35 events are selected in the *photon* sample.

We prepare three DCA distribution templates: the *non-collision* template, the *misidentified jets* template, and the e/γ template. The first template is obtained by selecting events with no hard scatter (no reconstructed interaction vertex or total number of reconstructed tracks less than three), or events with identified cosmic muons. The *misidentified jets* template is extracted from the *fake photon* sample, which fulfills exactly the same requirements as the *photon* sample except that the photon track isolation requirement is inverted. This sample is dominated by misidentified jets. Finally, the e/γ template is obtained from a real data sample of isolated electrons.

The total number of background events from misidentified jets ($N_{\rm fake}$) can be predicted from the *fake photon* sample if one knows the rates at which jets, passing all other photon ID criteria, fail or pass the track isolation requirement. To measure those rates we use an *EM plus jet* sample, where the EM object passes all photon ID requirements except the track isolation, and where the jet approximately balances the EM object in the transverse plane. We first determine the number of events (N_1) in the sample that fail the track isolation requirement. We then examine the DCA distribution for events that pass the track isolation, and exploit the difference in DCA distributions of real and misidentified photons to extract the number of the latter passing the track isolation (N_2). $N_{\rm fake}$ is then equal to the number of events in the *fake photon* sample multiplied by N_2/N_1. We fit the *photon* sample DCA distribution to a linear sum of the three templates, fixing the contribution of *misidentified jets* as described above, and determine the e/γ and *non-collision* contributions. The result of the fit is illustrated in Fig. 1. Most of the signal photons are within 4 cm in DCA, therefore we limit our analysis to this particular window which contains 29 data events.

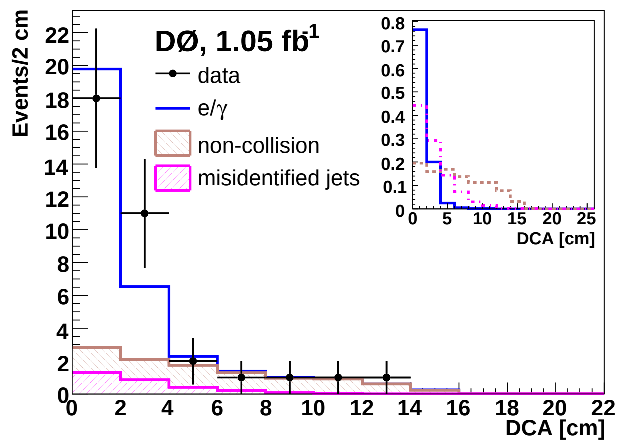

FIG. 1: Template fit in DCA of the selected events in data. Inset plot displays individual template shapes.

The only physics background to the $\gamma + \not\!\!E_T$ final state comes from the process $Z + \gamma \to \nu\overline{\nu} + \gamma$. This irreducible contribution is estimated from a sample generated with PYTHIA [12] using CTEQ6L1 parton distribution functions (PDF) [13]. The main instrumental background arises from $W \to e\nu$ decays, where the electron, due to tracking inefficiency or hard bremsstrahlung, is misidentified as a photon. This contribution is estimated from data using a sample of isolated electrons. The same requirements as for the *photon* sample are imposed, and the remaining number of events is scaled by $(1 - \epsilon_{\rm trk})/\epsilon_{\rm trk}$, where $\epsilon_{\rm trk}$ is the track reconstruction efficiency determined to be $(98.6 \pm 0.1)\%$ [14]. A smaller instrumental contribution to the background is expected from $W + \gamma$ production where the charged lepton in a leptonic W boson decay is not detected. The kinematics of this contribution is obtained from $W(+\text{jets}) \to \text{lepton} + \nu(+\text{jets})$ Monte Carlo (MC) samples generated with PYTHIA, while the cross section is taken from the MC generator based on [15], which predicts all contributions (initial state radiation, trilinear gauge boson vertex, and final state radiation) to the full process. We generate signal events [16] with $M_D = 1.5$ TeV for $n = 2, 3, 4, 5, 6, 7$ and 8. For different values of M_D, the cross section scales as $1/M_D^{n+2}$, leaving the kinematic spectra unaffected for a fixed number of extra dimensions.

All MC events are passed through a detector simulation based on the GEANT [17] package, and processed using the same reconstruction software as for the data. Additionally, we apply scale factors which account for the differences between the efficiency determinations from data and simulation.

TABLE I: Data and estimated backgrounds.

Background	Number of expected events
$Z+\gamma \to \nu\bar{\nu}+\gamma$	12.1 ± 1.3
$W \to e\nu$	3.8 ± 0.3
Non-collision	2.8 ± 1.4
Misidentified jets	2.2 ± 1.5
$W+\gamma$	1.5 ± 0.2
Total Background	22.4 ± 2.5
Data	29

The main sources of systematic error are the uncertainty in the photon identification efficiency (5%), the uncertainty in the total integrated luminosity (6.1%), and 4% uncertainty from the PDF. For the case of SM backgrounds estimated from MC, the quoted errors include the uncertainty on the cross sections, which is dominated by the uncertainty in the k-factors (7%) [15, 18]. The uncertainty in the width of the e/γ sample DCA template results in an additional systematic error of 0.4 events in the non-collision background estimate.

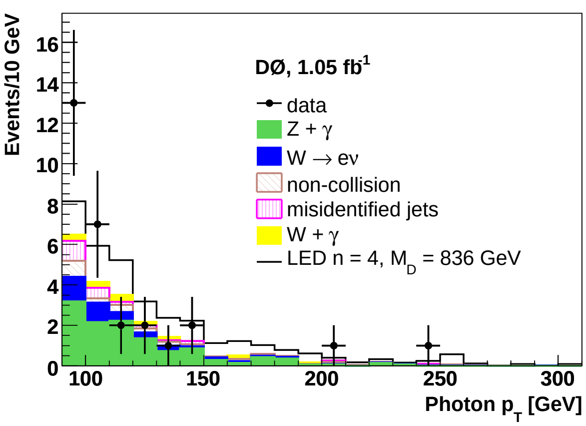

FIG. 2: Photon p_T distribution for the final candidate events, after all the applied requirements. The LED signal is stacked on top of SM backgrounds.

The final number of events for data and backgrounds are given in Table I. Fig. 2 shows the photon p_T distribution, with the SM backgrounds stacked on top of each other. Data and the SM expectation agree, so we proceed to set lower limits for the fundamental Planck scale M_D. We employ the Modified Frequentist approach [19] to set limits on the production cross section. This method is based on a log-likelihood ratio test statistic and uses the binned photon p_T distribution. At the 95% C.L. we find the following lower limits: $M_D > 884$, 864, 836, 820, 797, 797 and 778 GeV for $n = 2$, 3, 4, 5, 6, 7 and 8 extra dimensions, respectively. Table II and Fig. 3 summarize the the results for the limit calculations.

To conclude, we have conducted a search for LED in the $\gamma+\not\!\!E_T$ channel, finding no evidence for their presence. We have set limits on the fundamental Planck scale, significantly improving results of previous searches.

TABLE II: Summary of limit calculations.

n	Signal efficiency	Observed (expected) cross section limit (fb)	Observed (expected) M_D lower limit (GeV)
2	0.49 ± 0.04	27.6 (23.4)	884 (921)
3	0.48 ± 0.04	24.5 (22.7)	864 (877)
4	0.47 ± 0.04	25.0 (22.8)	836 (848)
5	0.43 ± 0.04	25.0 (24.8)	820 (821)
6	0.50 ± 0.05	25.4 (22.3)	797 (810)
7	0.49 ± 0.04	24.0 (23.1)	797 (801)
8	0.52 ± 0.05	24.2 (21.9)	778 (786)

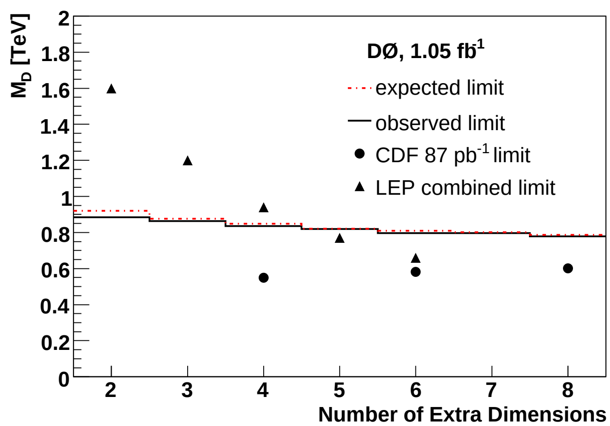

FIG. 3: Expected and observed lower limits on M_D for LED in the $\gamma+\not\!\!E_T$ final state. CDF limits with 87 pb^{-1} of data [3], and LEP combined limits [6] are also shown. The data are the black points with statistical uncertainties.

We thank Stephen Mrenna for his help with generating MC signal events, the staffs at Fermilab and collaborating institutions, and acknowledge support from the DOE and NSF (USA); CEA and CNRS/IN2P3 (France); FASI, Rosatom and RFBR (Russia); CNPq, FAPERJ, FAPESP and FUNDUNESP (Brazil); DAE and DST (India); Colciencias (Colombia); CONACyT (Mexico); KRF and KOSEF (Korea); CONICET and UBACyT (Argentina); FOM (The Netherlands); STFC (United Kingdom); MSMT and GACR (Czech Republic); CRC Program, CFI, NSERC and WestGrid Project (Canada); BMBF and DFG (Germany); SFI (Ireland); The Swedish Research Council (Sweden); CAS and CNSF (China); and the Alexander von Humboldt Foundation.

[a] Visitor from Augustana College, Sioux Falls, SD, USA.

[b] Visitor from The University of Liverpool, Liverpool, UK.
[c] Visitor from ICN-UNAM, Mexico City, Mexico.
[d] Visitor from II. Physikalisches Institut, Georg-August-University, Göttingen, Germany.
[e] Visitor from Helsinki Institute of Physics, Helsinki, Finland.
[f] Visitor from Universität Zürich, Zürich, Switzerland.
[‡] Deceased.

[1] N. Arkani-Hamed, S. Dimopoulus, G. Dvali, Phys. Lett. B **429**, 263 (1998).
[2] G. Guidice, R. Rattazzi, and J. Wells, Nucl. Phys. **B544**, 3 (1999).
[3] D. Acosta *et al.* (CDF Collaboration), Phys. Rev. Lett. **89**, 281801 (2002).
[4] B. Abbott *et al.* (D0 Collaboration), Phys. Rev. Lett. **86**, 1156 (2001); Ibid **90**, 251802 (2003); Ibid **95**, 161602 (2005).
[5] D. Acosta *et al.* (CDF Collaboration), Phys. Rev. Lett. **92**, 121802 (2004).
[6] LEP Exotica Working Group, URL: `http://lepexotica.web.cern.ch/LEPEXOTICA/notes/2004-03/ed_note_final.ps.gz`, and references therein.
[7] V.M. Abazov *et al.* (D0 Collaboration), Nucl. Instrum. Methods Phys. Res. A **565**, 463 (2006).
[8] Pseudorapidity is defined as $-\ln[\tan(\theta/2)]$, where θ is the angle between the particle and the proton beam direction.
[9] S. Abachi *et al.* (D0 Collaboration), Nucl. Instrum. Methods Phys. Res. A **338**, 185 (1994).
[10] T. Andeen *et al.*, FERMILAB-TM-2365 (2006).
[11] G. C. Blazey *et al.*, arXiv:hep-ex/0005012 (2000).
[12] T. Sjöstrand *et al.*, Comput. Phys. Commun. **135**, 238 (2001).
[13] J. Pumplin *et al.*, JHEP **0207**, 012 (2002); D. Stump *et al.*, JHEP **0310**, 046 (2003).
[14] V.M. Abazov *et al.* (D0 Collaboration), Phys. Lett. B **659**, 856 (2008).
[15] U. Baur and E.L. Berger, Phys. Rev. D **41**, 1476 (1990).
[16] Stephen Mrenna, private communications.
[17] R. Brun and F. Carminati, CERN Program Library Long Writeup W5013, 1994.
[18] U. Baur, T. Han, and J Ohnemus, Phys. Rev D **57**, 2823 (1998); The k-factor, when the analysis requirements are applied, varies from ≈ 1.05 for photons with $p_T = 50$ GeV to ≈ 0.95 for photons with $p_T = 250$ GeV.
[19] W. Fisher, FERMILAB-TM-2386-E (2007); T. Junk, Nucl. Instrum. Methods Phys. Res. A **434**, 435 (1999); A. Read, CERN 2000-005 (2000).